

1
2
3 **Structural and chemical reactivity modifications of a cobalt perovskite**
4 **induced by Sr-substitution. An in situ XAS study.**
5
6

7
8 *Jose L. Hueso, Juan P. Holgado, Rosa Pereñíguez, V.M. Gonzalez-DelaCruz and*
9

10 *Alfonso Caballero**
11

12
13
14
15 *Instituto de Ciencia de Materiales de Sevilla (CSIC-University of Sevilla) and*
16
17 *Departamento de Química Inorganica, Universidad de Sevilla. Avda. Américo*
18 *Vespucio, 49. 41092. Seville, Spain.*
19
20
21
22
23
24

25 **Abstract**
26

27 LaCoO₃ and La_{0.5}Sr_{0.5}CoO_{3-δ} perovskites have been studied by *in situ* Co K-
28 edge XAS. Although the partial substitution of La(III) by Sr(II) species induces an
29 important increase in the catalytic oxidation activity and modifies the electronic state of
30 the perovskite, no changes could be detected in the oxidation state of cobalt atoms. So,
31 maintaining the electroneutrality of the perovskite requires the generation of oxygen
32 vacancies in the network. The presence of these vacancies explains that the substituted
33 perovskite is now much more reducible than the original LaCoO₃ perovskite. As
34 detected by *in situ* XAS, after a consecutive reduction and oxidation treatment, the
35 original crystalline structure of the LaCoO₃ perovskite is maintained, although in a more
36 disordered state, which is not the case for the Sr doped perovskite. So, the
37 La_{0.5}Sr_{0.5}CoO_{3-δ} perovskite submitted to the same hydrogen reduction treatment
38 produces metallic cobalt, while as determined by *in situ* XAS spectroscopy the
39 subsequent oxidation treatment yields a Co(III) oxide phase with spinel structure.
40 Surprisingly, no Co(II) species are detected in this new spinel phase.
41
42
43
44
45
46
47
48
49
50
51
52
53
54
55
56
57
58
59
60
61
62
63
64
65

1
2 **Keywords:**
3

4 Inorganic compounds; XAFS (EXAFS and XANES); crystal structure; chemical
5
6 techniques
7
8
9

10 **Corresponding Author**
11

12 * E-mail: caballero@us.es
13
14
15
16
17
18
19
20

21 **1. Introduction**
22

23 Oxides with perovskite structure (ABO_3) are of interest because of their electric,
24 magnetic and, especially, its outstanding properties as oxidation catalysts (1-7). In
25 particular, a previous work from our group (8) showed as these perovskite present a
26 high oxidation activity, especially when Sr cations are incorporated in the structure.
27
28 Additionally, many papers have been published about Sr doped cobaltites, and some
29 authors have found that the spin configuration of the $LaCoO_3$ changes by introducing
30 Sr(II) atoms (9-11). But there is no agreement about the origin of these new physical
31 and chemical characteristics: formation of Co(IV) ions or oxygen vacancies (12,13). In
32 a previous work (14), we have shown as the Sr(II) cations modify the spin state because
33 of differences in sizes and generation of oxygen vacancies. In some cases, especially for
34 catalytic applications, these solids need to be transformed by hydrogen reduction at high
35 temperature. These reduction treatment of these ABO_3 phases performed under
36 controlled reduction conditions can produce a well-dispersed transition metal B on a
37 matrix comprising the A_2O_3 oxide phase as a support (Co/La_2O_3 in our case). So,
38 knowing how the presence of Sr on the original perovskite phase modified the effect of
39 the reduction treatment, changing the temperature of the process but also the state of the
40
41
42
43
44
45
46
47
48
49
50
51
52
53
54
55
56
57
58
59
60
61
62
63
64
65

1 reduced transition metal dispersed on the support is a main goal for the application of
2 these materials. With this purpose, herein, we have investigated by means of *in situ* X-
3 ray absorption spectroscopy (XAS) at the Co K-edge, the reduction process of these two
4 perovskites, $\text{La}_{0.5}\text{Sr}_{0.5}\text{CoO}_{3-\delta}$ and LaCoO_3 , paying special attention to any changes
5 induced in the structure and chemical reactivity of the Strontium-substituted cobalt
6 perovskite after high temperature reduction and oxidation treatment.
7
8
9
10
11
12
13
14
15
16

17 **2. Experimental**

18 2.1. Preparation of solids

19 The two cobaltites, $\text{La}_{0.5}\text{Sr}_{0.5}\text{CoO}_{3-\delta}$ and LaCoO_3 were synthesized by a spray
20 pyrolysis methodology described elsewhere (15,16). Previously, 0.1 M solution
21 containing $\text{La}(\text{NO}_3)_3 \cdot 6\text{H}_2\text{O}$ (99.99%, Aldrich), $\text{Co}(\text{NO}_3)_2 \cdot 6\text{H}_2\text{O}$ (>98%, Fluka), and
22 $\text{Sr}(\text{NO}_3)_2$ (>99%, Fluka) were prepared and used as precursors. After nebulization, the
23 precursors were introduced into two consecutive online furnaces, at 250 and 600°C,
24 respectively. At the end, amorphous powders of the solids were collected. After an
25 annealing treatment at 600°C for 4 h, these amorphous powders supplied LaCoO_3 and
26 $\text{La}_{0.5}\text{Sr}_{0.5}\text{CoO}_{3-\delta}$ crystalline perovskites with rhombohedral structures (16).
27
28
29
30
31
32
33
34
35
36
37
38
39
40
41
42
43

44 2.2. Characterization techniques

45 XRD patterns of the samples were recorded using a Siemens D-500
46 diffractometer, working in a Bragg-Bentano configuration, with a Cu anode, and
47 applying a voltage of 36 kV and a current of 26 mA. A step size of 0.02 degrees and an
48 accumulation time of 10 s per step were used for the scans.
49
50
51
52
53
54
55

56 The Temperature Programmed Reduction (TPR) experiments were made using a
57 5% H_2/Ar gas mixture (50 ml/min total flow) up to 750°C with a heating rate of 10
58
59
60
61
62
63
64
65

1 K/min. As previously described, the experimental conditions were chosen to assure that
2 no peaks coalescence occurs (17). H₂ consumption was registered by means of a thermal
3 conductivity detector (TCD) pre-calibrated using CuO. Also, a mass spectrometer in
4 line with the TCD, previously calibrated with reference mixtures, was used to detect
5 variations of hydrogen concentration and possible sub-products formation.
6
7
8
9
10

11 The X-ray absorption spectra (XAS) were recorded at the BM25 beam line
12 (SPLINE) of the ESRF synchrotron (Grenoble, France). The spectra were acquired at
13 the Co K-edge in transmission mode using a suitably modified commercial infrared cell
14 (Specac), and self-supported wafers of the perovskite samples prepared using the
15 optimum weight to maximize the signal-to-noise ratio in the ionization chambers (log
16 $I_0/I_1 \approx 1$). Both, the EXAFS and XANES regions of the XAS spectra were collected
17 after the corresponding treatments. For the thermal treatments a set of mass flow
18 controllers were used for dosing the gases to the cell, with a total flow of 100 ml/min. In
19 all cases, the gas mixtures used for the hydrogen reduction and reoxidation treatments
20 (H₂, 500°C, 30'; O₂, 500°C, 30') were the same to those described in the TPR
21 experiments. A standard Co foil was introduced for energy calibration after the second
22 ionization chamber (*I1*) and measured simultaneously. Typically, the XAS spectra of Co
23 K-edge were recorded from 7500 to 8700 eV, with a variable step energy value, with a
24 minimum 0.5 eV step across the XANES region. After mathematical extraction from
25 the XAS spectra, the EXAFS oscillations were Fourier transformed in the range 2.0–
26 12.0 Å⁻¹. Reference spectra for CoO, Co₃O₄ and metallic Co were recorded using
27 standard reference samples.
28
29
30
31
32
33
34
35
36
37
38
39
40
41
42
43
44
45
46
47
48
49
50
51
52
53
54
55

56 **3. Results and Discussion**

57 **3.1. Structural and chemical characterization of cobaltites**

58
59
60
61
62
63
64
65

1
2
3
4
5
6
7
8
9
10
11
12
13
14
15
16
17
18
19
20
21
22
23
24
25
26
27
28
29
30
31
32
33
34
35
36
37
38
39
40
41
42
43
44
45
46
47
48
49
50
51
52
53
54
55
56
57
58
59
60
61
62
63
64
65

The two perovskite samples, LaCoO_3 and $\text{La}_{0.5}\text{Sr}_{0.5}\text{CoO}_{3-\delta}$, prepared by spray pyrolysis and calcined at 600°C present rhombohedral structures (R-3c), as determined by XRD (15). Also, as shown in a previous publication (14), after calcination the XANES spectra (Figure 1a) and the Fourier Transform (F.T.) of the EXAFS region (Figure 1b) of the Co K-edge XAS spectra are typical for perovskite structure (6,11,12). Moreover, the XANES spectra are clearly different from the two cobalt oxide references, Co_3O_4 and CoO , also included in the Figure 1. The higher energy of the edges of both cobalt perovskites indicates a higher oxidation state of cobalt than in the references, which must correspond to Co(III) species. As this energy is the same for both perovskite samples, and the oxidation state of cobalt in the LaCoO_3 solid can be unambiguously assigned to Co(III) species, this similarity in the edge energy can be taken as an evidence for the absence of Co(IV) species in the Sr-substituted sample. Although some authors claim the existence of Co(IV) ions in this kind of substituted perovskites (18), this fact allows us to conclude that oxygen vacancies must be distributed in the structure in order to compensate the different cationic charge between La(III) and Sr(II). So, considering that no Co(IV) species are present in the Sr-substituted solid, differences in charge between Sr (2+) and La (3+) must be reflected in a number of oxygen vacancies corresponding to a stoichiometric δ value of 0.25, that is $\text{La}_{0.5}\text{Sr}_{0.5}\text{CoO}_{2.75}$.

As mentioned above, the F.T. magnitude of the EXAFS spectra (Figure 1b), is similar to those reported previously for perovskite structures (11). Differences in intensity for the overlapping peaks in the 3-4 Å range, higher for the LaCoO_3 , can be explained considering the structural disorder caused by the presence of oxygen vacancies in the Sr-containing sample and/or by interferences between the EXAFS oscillation components coming from Sr and La in the second coordination shell (14).

3.2. Reactivity changes induced by Sr

As mentioned before, the insertion of Sr(II) atoms in the “A” position of ABO_3 perovskites was primarily intended to increase the catalytic reactivity of the original $LaCoO_3$ cobaltite by inducing changes in the cobalt oxidation state and/or the formation of oxygen vacancies, as a result of the presence of Sr(II) species substituting the La(III) atoms. In a previous paper (8), we have showed as the $LaCoO_3$ perovskite presents an important activity for the thermal oxidation of carbon, producing a decrease in its temperature of combustion of ca. 150°C and a significant increase in the selectivity toward CO_2 . When Sr cations are incorporated, a further 30°C decrease in the combustion temperature is observed. Also, the selectivity to CO_2 increases from 89 to 94%. So, it is clear that incorporation of Sr(II) cations modified the catalytic performance of the cobalt perovskite. Differences in reactivity have also become evident in the TPR profiles included in Figure 2. After calcination at 500°C , the profile of the Sr-containing sample presents two main peaks centered at 355 and 450°C , respectively. The reduction process is completed at 500°C , when the perovskite structure collapse as the cobalt is completely reduced, as deduced from the TPR profile. This fact has been verified by XRD (not included). On the contrary, the $LaCoO_3$ presents two main peaks at higher temperature (420 and 550°C), and need to be heated in hydrogen at 600°C to complete the reduction process. To further elucidate the structural and chemical changes involved in these reduction and reoxidation treatments, an *in situ* XAS study has been accomplished over these two cobaltites.

Figure 3a shows the XANES spectra for the $LaCoO_3$ sample submitted to a reduction treatment in hydrogen at 500°C , followed by a reoxidation at the same temperature. It can be observed as upon reduction, the edge of the XANES spectrum is

1 shifted to lower energy, but higher than that of CoO, indicating that the cobalt has been
2 only partially reduced to Co(II) species. However, no important changes can be
3
4 observed in the oscillation pattern after the edge, showing that no major structural
5
6 changes have occurred in the perovskite structure. So, these results are compatible with
7
8 a partially reduced cobalt perovskite, where the network are basically maintained, but
9
10 containing Co(II) and oxygen vacancies species. After reoxidation at 500°C almost an
11
12 identical XANES spectrum is obtained (Figure 3a) to the original LaCoO₃ sample and
13
14 showed same edge energy. The magnitude of the F.T. peaks from the EXAFS spectra
15
16 (Figure 3b) brings about the same conclusions, with also new insights into the structural
17
18 state of the treated perovskite. So, after reduction at 500°C the F.T. maintains the same
19
20 peaks with the same original R values, although the intensity is much lower. These
21
22 results show once again that the original crystallographic structure remains after the
23
24 hydrogen treatment at 500°C. However, while maintaining the structure, this treatment
25
26 causes an increase in the structural disorder, which is reflected in less intense peaks in
27
28 the F.T. The subsequent reoxidation at 500°C restores the intensity of the first peak (Co-
29
30 O first coordination shell), while the peaks around 3-4Å are only slightly recovered,
31
32 reaching an intensity similar to the Sr-substituted perovskites FT included in Figure 1b.
33
34 So, XAS spectroscopy shows as cobalt is partially reduced to Co(II) but the perovskite
35
36 framework remains unchanged. After reoxidation the Co(III) state is recovered but a
37
38 completely ordered perovskite network is not fully restored.

39
40
41 As expected from the TPR profile of Figure 2, the XANES spectra (Figure 4a)
42
43 indicates that the Sr-substituted cobaltite is almost completely reduced to the metallic
44
45 state upon treatment in hydrogen at 500°C. Also, the main peak at 2.2Å in the F.T.
46
47 (Figure 4b) appears at the same position that Co-Co distances of metallic cobalt (not
48
49 shown), and only the weak shoulder at 1.6Å, coming from Co-O distances (see Co₃O₄
50
51
52
53
54
55
56
57
58
59
60
61
62
63
64
65

1 F.T. in Figure 4b), reveals some remains of oxidized cobalt. Remarkably, the
2 subsequent reoxidation treatment produces a cobalt oxide phase with notable differences
3 and resemblances with the reference of massive cobalt spinel Co_3O_4 . So, while the F.T.
4 shows a radial distribution function similar to the cobalt spinel, with three main peaks
5 centered at 1.45, 2.48 and 3.02Å (without phase correction), the XANES indicates that
6 cobalt in the Sr-containing perovskite is much more oxidized than the cobalt spinel,
7 according to the higher energy of the edge shown in Figure 4a. However, in agreement
8 with the F.T. results of Figure 4b, the oscillations after the edge are similar to that of the
9 cobalt spinel used as a reference. These findings show that a highly oxidized spinel
10 structure is stabilized after this reduction and reoxidation treatments. It is important to
11 stress at this stage that, according to the XRD diagrams included in Figure 5, the
12 reduced and oxidized sample is mainly amorphous (note that right diagram is amplified
13 by 3). The small remaining peaks are related to a crystalline perovskite phase and only
14 very weak peaks from a (conventional) spinel phase can be detected. So, and according
15 to the previous Co K-edge XAS data, most of the solids is present as an amorphous
16 spinel-like phase.
17
18
19
20
21
22
23
24
25
26
27
28
29
30
31
32
33
34
35
36
37
38
39
40

41 **4. Conclusions**

42
43 In summary, we have presented an *in situ* XAS study at the Co K-edge of
44 LaCoO_3 and $\text{La}_{0.5}\text{Sr}_{0.5}\text{CoO}_{3-\delta}$ perovskites submitted to some calcination and reduction
45 treatments. The results have allowed us to conclude that partial substitution of La(III)
46 cations by Sr(II) divalent species produces important changes in the chemical reactivity.
47
48 As no changes could be detected in the oxidation state of cobalt atoms, oxygen
49 vacancies must be stabilized in the perovskite network, strongly modifying the
50 reactivity of the perovskite, now more reducible by a hydrogen treatment. Surprisingly,
51
52
53
54
55
56
57
58
59
60
61
62
63
64
65

1
2
3
4
5
6
7
8
9
10
11
12
13
14
15
16
17
18
19
20
21
22
23
24
25
26
27
28
29
30
31
32
33
34
35
36
37
38
39
40
41
42
43
44
45
46
47
48
49
50
51
52
53
54
55
56
57
58
59
60
61
62
63
64
65

it have been observed that, by reoxidation of the previously reduced $\text{La}_{0.5}\text{Sr}_{0.5}\text{CoO}_{3-\delta}$, a highly oxidized amorphous spinel-like phase has been obtained, containing just Co(III) species, with no Co(II) as it is the case in the massive cobalt spinel.

Acknowledgements

We thank the Ministry of Science and Education of Spain for financial support (Project ENE2011-24412). We also thank the staff of the ESRF BM25 beamline and ESRF facility (Grenoble, France) for funding and helping to accomplish these experiments.

References

- (1) Sugiura, Y.; Mukai, D. *Int.J.Hydr.Energy* **2013**, *38*, 7822-7829.
- (2) Nishihata, Y.; Mizuki, J.; Akao, T.; Tanaka, H.; Uenishi, M.; Kimura, M.; Okamoto, T.; Hamada, N. *Nature* **2002**, *418*, 164-167.
- (3) Itoh, T.; Nakayama, M. *JSSC* **2012**, *192*, 38-46.
- (4) Kim, J.; Lee, H. *Materials Letters* **2013**, *92*, 39-41.
- (5) Rijssenbeek, J. T.; Saito, T.; Malo, S.; Azuma, M.; Takano, M.; Poeppelmeier, K. R. *J. Am. Chem. Soc.* **2005**, *127*, 675-681.
- (6) Toulemonde, O.; N`Guyen, N.; Studer, F. *JSSC* **2001**, *158*, 208-217.
- (7) Lu, Y.; Eyssler, A.; Otal, E. H.; Matam, S. K.; Brunko, O.; Weidenkaff, A.; Ferri, D. *Catal. Today* **2013**, *208*, 42-47.
- (8) Hueso, J. L.; Caballero, A.; Ocaña, M.; Gonzalez-Eliphe, A. R. *J. Catal.* **2008**, *257*, 334-344.
- (9) Abbate, M.; Fuggle, J. C.; Fujimori, A.; Tjeng, L. H.; Chen, C. T.; Potze, R.; Sawatzky, G. A.; Eisaki, H.; Uchida, S. *Phys. Rev. B* **1993**, *47*, 16124-16130.

- 1
2
3
4
5
6
7
8
9
10
11
12
13
14
15
16
17
18
19
20
21
22
23
24
25
26
27
28
29
30
31
32
33
34
35
36
37
38
39
40
41
42
43
44
45
46
47
48
49
50
51
52
53
54
55
56
57
58
59
60
61
62
63
64
65
- (10) Pinta, C.; Fuchs, D.; Merz, M.; Wissinger, M.; Arac, E.; Löhneysen, H. v.; Samartsev, A. *Phys. Rev. B* **2008**, *78*, 174402.
- (11) Haas, O.; Ludwig, C.; Bergmann, U.; Singh, R.N.; Braun, A.; Graule, T. *JSSC* **2011**, *184*, 3163-3171.
- (12) Hanashima, T.; Azuhata, S.; Yamawaki, K.; Shimizu, N.; Mori, T. Tanaka, M.; Sasaki, S. *Jap. J. Appl. Phys.* **2004**, *43*, 4171-4178.
- (13) Komo, M.; Hagiwara, A.; Taminato, S.; Hirayama, M.; Kanno, R. *Electrochemistry* **2012**, *80*, 834-838.
- (14) Hueso, J. L.; Holgado, J.P.; Pereñíguez, R.; Mun, S.; Salmeron, M.; Caballero, A. *JSSC* **2010**, *183*, 27-32.
- (15) Hueso, J. L.; Cotrino, J.; Caballero, A.; Espinos, J. P.; Gonzalez-Elipe, A. R. *J. Catal.* **2007**, *247*, 288-297.
- (16) Lopez-Navarrete, E.; Caballero, A.; Orera, V. M.; Lazaro, F. J.; Ocaña, M. *Acta Mater.* **2003**, *51*, 2371-2381.
- (17) Malet, P.; Caballero, A. *J. Chem. Soc. Faraday Trans.* **1988**, *84*, 2369-2375.
- (18) Berry, F. J.; Marco, J.F.; Ren, X. *J. Sol. State Chem.* **2005**, *178*, 961-969.

Figure captions

Figure 1. Co K-edge XANES spectra (a) and F.T. of the EXAFS region (b) of Lanthanum Cobaltites calcined at 600°C.

Figure 2. Temperature-programmed reduction (TPR) profiles of Lanthanum Cobaltites calcined at 600°C.

Figure 3. *In situ* Co K-edge XANES spectra (a) and F.T. of the EXAFS region (b) of LaCoO₃ submitted to the indicated treatments.

Figure 4. *In situ* Co K-edge XANES spectra (a) and F.T. of the EXAFS region (b) of La_{0.5}Sr_{0.5}CoO_{3-δ} submitted to the indicated treatments.

Figure 5. XRD diagrams of La_{0.5}Sr_{0.5}CoO_{3-δ} calcined at 600°C (left) and reoxidized after reduction at 500°C (right).

Figure 1
[Click here to download high resolution image](#)

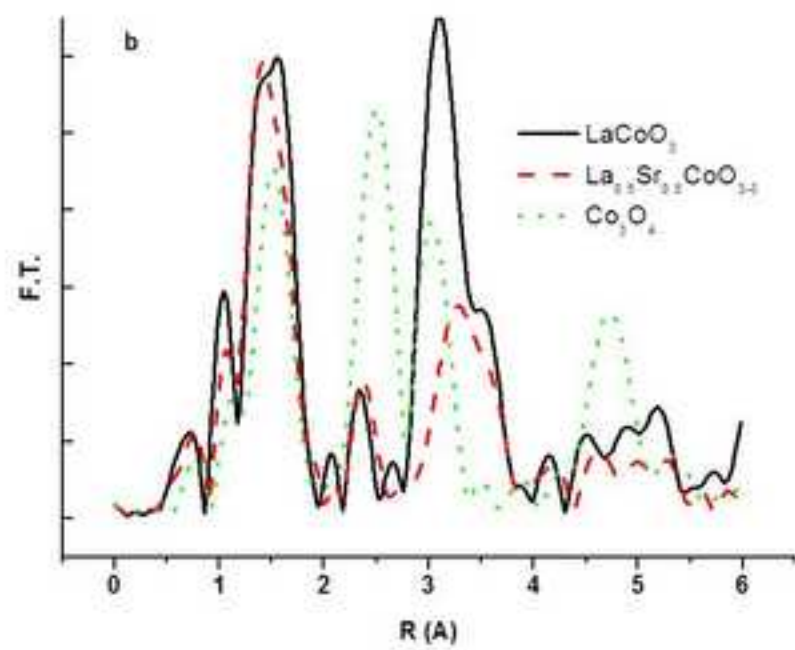
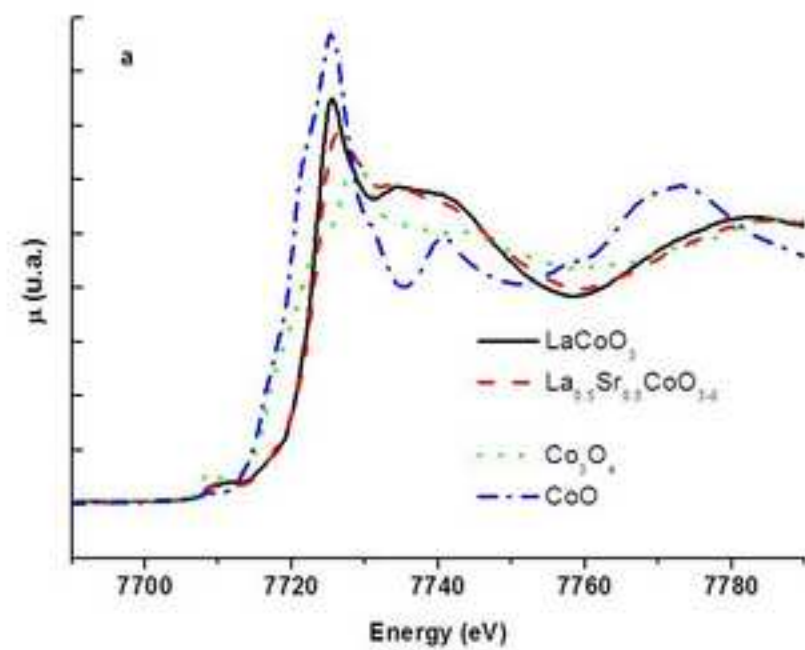


Figure 2
[Click here to download high resolution image](#)

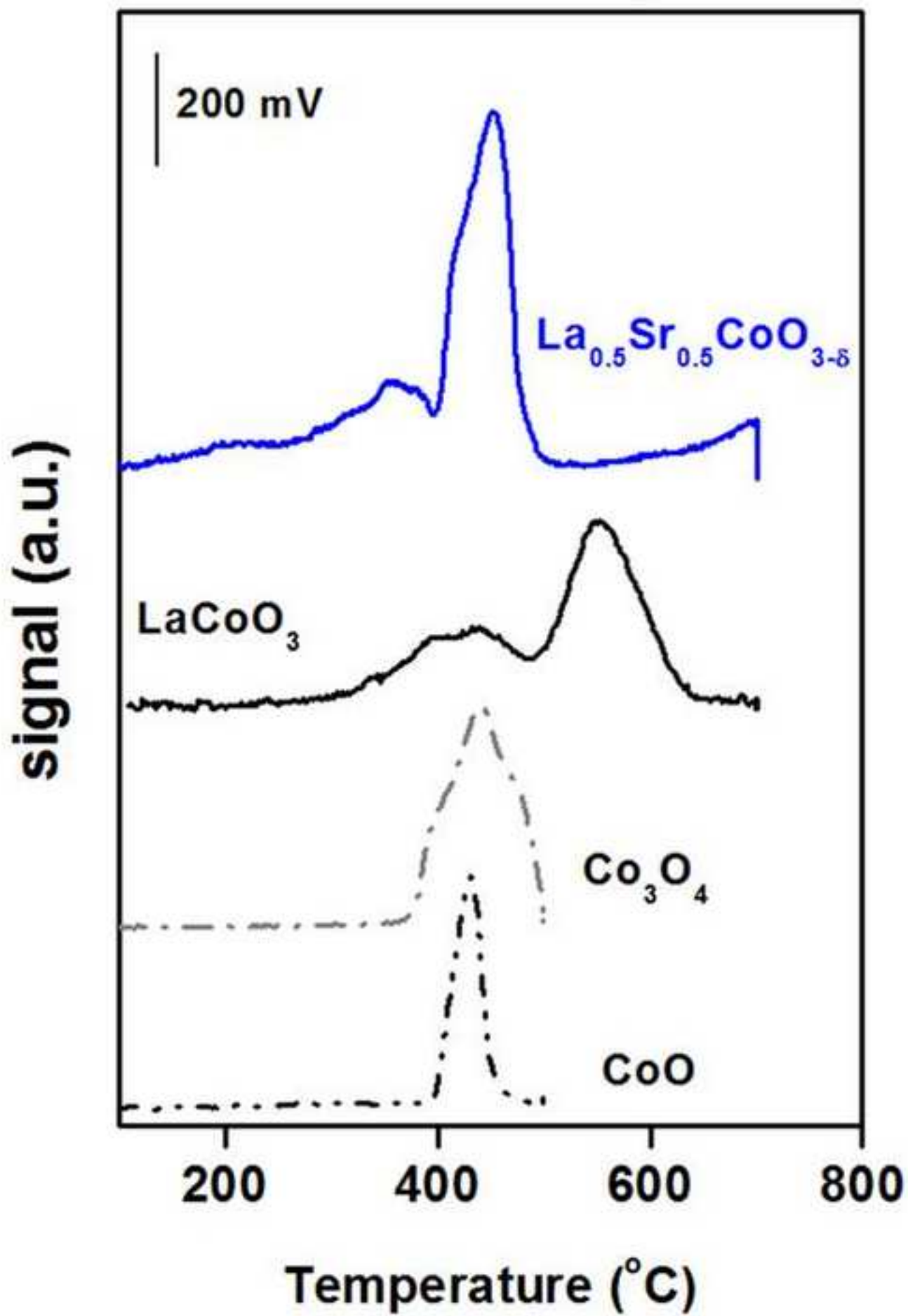


Figure 3
[Click here to download high resolution image](#)

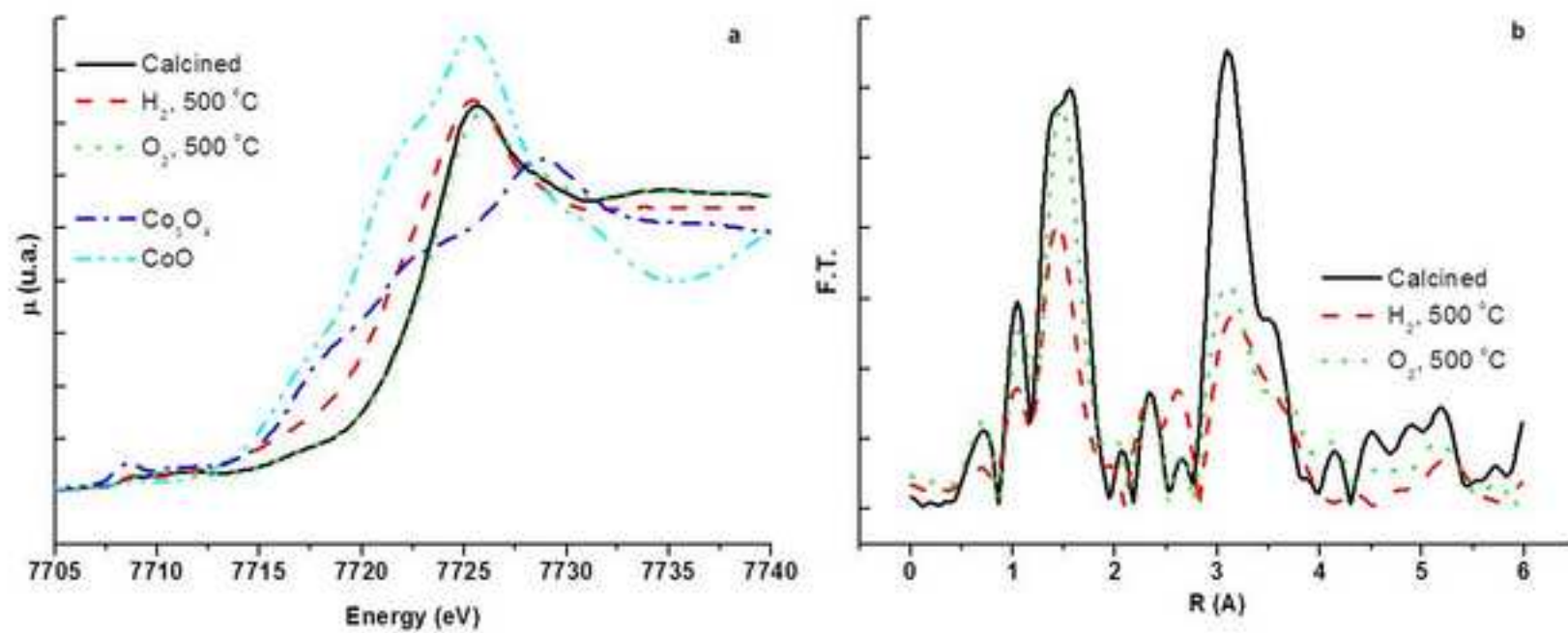


Figure 4
[Click here to download high resolution image](#)

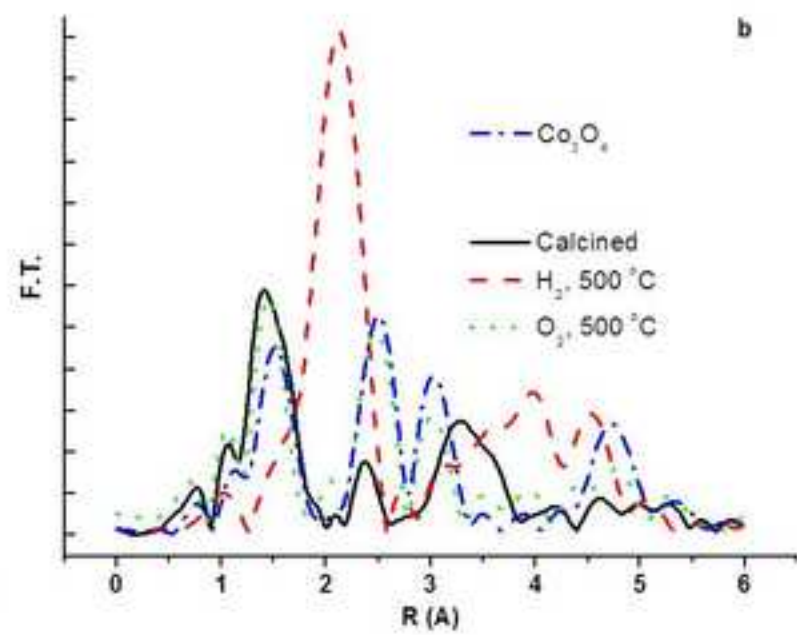
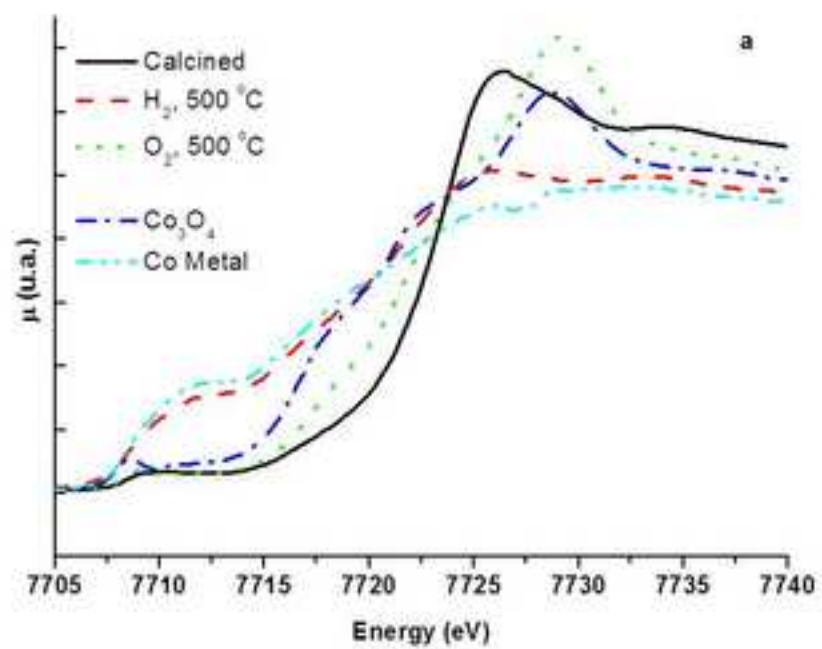


Figure 5
[Click here to download high resolution image](#)

